NANOPARTICLES AND OCCUPATIONAL HEALTH

Dustiness behaviour of loose and compacted Bentonite and organoclay powders: What is the difference in exposure risk?

Keld Alstrup Jensen · Ismo Kalevi Koponen · Per Axel Clausen · Thomas Schneider

Abstract Single-drop and rotating drum dustiness testing was used to investigate the dustiness of loose and compacted montmorillonite (Bentonite) and an organoclay (Nanofil®5), which had been modified from montmorillonite-rich Bentonite. The dustiness was analysed based on filter measurements as well as particle size distributions, the particle generation rate, and the total number of generated particles. Particle monitoring was completed using a TSI Fast Mobility Particle Sizer (FMPS) and a TSI Aerosol Particle Sizer (APS) at 1 s resolution. Low-pressure uniaxial powder compaction of the starting materials showed a logarithmic compaction curve and samples subjected to 3.5 kg/cm^2 were used for dustiness testing to evaluate the role of powder compaction, which could occur in powders from large shipments or high-volume storage facilities. The dustiness tests showed intermediate dustiness indices (1,077–2,077 mg/kg powder) in tests of Nanofil®5, Bentonite, and compacted Bentonite, while a high-level dustiness index was found for compacted Nanofil®5 (3,487 mg/kg powder). All powders produced multimodal particle size-distributions in the dust cloud with one mode around 300 nm (Bentonite) or 400 nm (Nanofil®5) as well as one (Nanofil®5) or two modes (Bentonite) with peaks between 1 and 2.5 μm. The dust release was found to occur either as a burst (loose Bentonite and Nanofil®5), constant rate (compacted Nanofil®5), or slowly increasing rate (compacted Bentonite). In rotating drum experiments, the number of particles generated in the FMPS and APS size-ranges were in general agreement with the mass-based dustiness index, but the same order was not observed in the single-drop tests. Compaction of Bentonite reduced the number of generated particles with app. 70 and 40% during single-drop and rotating drum dustiness tests, respectively. Compaction of Nanofil®5 reduced the dustiness in the single-drop test, but it was more than doubled in the rotating drum test. Physically relevant low-pressure compaction may reduce the risk of particle exposure if powders are handled in operations with few agitations such as pouring or tapping. Repeated agitation, e.g., mixing, of these compacted powders, would result in reduced (app. 20% for Bentonite) or highly increased (app. 225% for Nanofil®5) dustiness and thereby alter the exposure risk significantly.

K. A. Jensen (✉) · I. K. Koponen · P. A. Clausen · T. Schneider
National Research Centre for the Working Environment, Lersø Parkallé 105, Copenhagen 2100, Denmark
e-mail: kaj@nrcwe.dk

Introduction

Scientific developments have opened numerous new potential applications of the technologically well-known clay minerals. Bentonite is one of the most common technical clay products and is the commercial name for a clay-rich material, which mainly consists of the monoclinic clay mineral montmorillonite from the di-octahedral smectite group. This so-called 2:1 layer clay contains an octahedral alumina or magnesia sheet between two tetrahedral silica sheets and can be described by the general structure formula:

$$(M_{x+y})_{0.33}(Al_{2-y}, Mg_y)_{4-6}(Si_{4-x}, Al_x)_4 O_{10}$$
$$(OH)_2 \cdot nH_2 O, \tag{1}$$
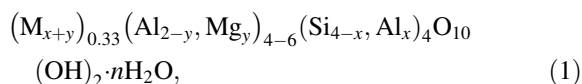
where M are charge-balancing interlayer cations, typically dominated by Na and Ca. Compositions with $y > x$ are true montmorillonite (Guven 1991).

Over the last decades, it has been found that chemical functionalization of montmorillonite can improve the miscibility and the technical performance in a range of products, such as cosmetics, paints, paper, lubricants, and remediation (e.g., Carrizosa et al. 2003; Patel et al. 2006; Konta 1995). During the recent years chemically modified clays have also been found to have high potential for the use as functional fillers in polymers (see e.g., Ray and Okamoto 2003). Usually, these modified clays are referred to as organoclays, nanoclays, or nanoflakes. They are produced by substituting the charge-balancing interlayer cations between the 2:1 magnesia-alumina-silicate sheets in the montmorillonite structure with cationic organic molecules, usually ammonium or phosphonium ions. The substitution causes delamination of the clay structure, resulting in single organically functionalised hexagonal magnesia-alumina-silicate platelets with a thickness on the order of 1 nm and a typical width of 100–200 nm (Ray and Okamoto 2003). For the use in polymer materials the organoclays may be functionalised with organophilic quarternary ammonium compounds. The final organoclay product is a high-porosity powder with a bulk density of around 0.40 to 0.50 g/cm^3 as compared to 0.35–0.87 g/cm^3 reported for various commercial Bentonites (Wieczorek et al. 2003; Heim et al. 2005).

The low bulk density of clay and organoclay powders and their loose nature suggest that such powders are easily dispersed. Consequently there may be a relatively high risk of exposure to air-borne particles during handling and dispersion of such powders in technological processes. Using a newly developed system for single-drop and rotating drum dustiness testing, it has recently been shown that the risk of particle exposure may be increased dramatically when changing from conventional powders to nanosize powders. In the case of TiO$_2$, the dustiness potential increased by a factor of 300 using either mass or particle number concentration analysis (Schneider and Jensen 2008). In the same study, clay powders (Bentonite and Talc) were found to have medium to high dustiness and on-line monitoring showed that most of the particles were released during an initial burst. Other particle types were found to have either a slowly decreasing or a constant particle generation rate. As for the case with TiO$_2$, introducing organoclays in a production may similarly result in increased risk of dust exposure as compared to the levels when using traditional Bentonite. Hence, application of organoclay does not only change the chemical composition of the exposure, but potentially also the particle size distribution and intensity of the exposure.

Powder dustiness and its kinetics may be controlled by a number of factors, such as the conditions during production, storage, and transport. A high humidity and long-term storage may cause intergranular fusion (caking) due to corrosion and local dissolution-precipitation processes (Szepvolgyi et al. 2001; Gbureck et al. 2005; Brockel et al. 2006). The physical conditions, including powder compaction during transport and storage, may be another important factor. Compaction changes the agglomeration or aggregation state of particles. Industrially, this effect is applied in granulation of powders to improve their appearance, flow, and mixing properties as well as to reduce the dustiness (see e.g., Freitag and Kleinebudde 2003; Tardos 2005; Nishii and Horio 2007). Despite the pressure exerted on a powder during storage and transport is expected to be much lower than the forces applied in the various granulation techniques (Takano and Horio 2004; Freitag and Kleinebudde 2003; Tien et al. 2007), low-pressure compaction may also change the particle generation behaviour during powder handling and the size distribution of the generated dust. These potential differences are apparently not investigated scientifically, but may play an important role in dustiness evaluation of powders.

In addition to these potential effects of compaction, assessments of exposure risk from dustiness

testing could benefit from a more detailed analysis of dustiness and the particle size distributions in the dust as function of a range of physicochemical storage conditions such as humidity, temperatures, and reaction kinetics. These factors may also unintentionally influence the exposure evaluations based on dustiness testing of a presumably representative powder, because the storage conditions of test samples in laboratories performing the tests may also influence the powder properties as compared to that of the original powder.

In this paper we investigate the dustiness, size distribution of the generated particles, and the particle generation kinetics of loose (as received) and compacted Bentonite and organoclay powders. For the study we employ a recently developed system for contemporaneously testing powder dustiness by single-drop and the continuous drop method (Schneider and Jensen 2008), which was modified from the recent EN standard 15051 (CEN 2006; Liden 2006).

Experimental

Samples and sample preparation

Dustiness tests were performed on loose Bentonite and organoclay as well as compacted samples of the same powders. Table 1 lists key data for the original powder materials. Previous X-ray diffraction analysis of the Bentonite sample has shown that the sample is very pure and consists entirely of 2:1 layer montmorillonite (Schneider and Jensen 2008). The functionalised organoclay (Nanofil®5) was obtained from Süd-Chemie AG (Moosburg, Germany) and consists of cation-exchanged Bentonite treated with dimethyl dialkyl (hydrogenated tallow, major chain length presumably C_{14}-C_{18}) ammonium salts and up to 0.5 wt% impurities of crystalline silica. The loss on ignition is ca. 35 wt%. Since organoclays are hydrophobic, the loss on ignition is assumed to be caused entirely by loss of the quarternary ammonium ions.

The original loose powders were tested as received, whereas the compacted powders were obtained after 5 min uniaxial pressure at 3.54 ± 0.14 kg/cm^2 under indoor laboratory temperature and humidity conditions. The compaction pressure could represent a potential maximum load on a powder during silo storage or large volume transport, but was selected

Table 1 Key specifications of the original powders tested

Material	XRD Phase abundance (wt%)	Crystallite size (nm)	Specific surface area (m^2/g^{-1})	Specific density (g/cm^3)	Bulk density (g cm^{-3})	Functionalization	CAS no.
Bentonite	100% montmorillonite	7.8[c]	NA	2.1 (2–3)	0.75[f]	None	52623-66-2
Nanofil®5[a]	>99.75% organoclay <0.25% crystalline silica[b]	1 × 100–500[d]	Ca. 750[e]	Ca. 1.8	0.4[f]	$^+N(CH_3)_2$(alkyl C14–18)$_2$	68953-58-2

[a] If nothing else stated, all data were obtained from the MSDS (material safety data sheet) for Nanofil® 5, SüdChemie A/S

[b] The organoclay was derived from Bentonite and has 35 wt% loss on ignition, which we assume to constitute the organic functionalization. The crystalline silica content makes <1% of the inhalable fraction and 3–5% of the alveolar dust, respectively

[c] Crystallite size along the crystallographic [001] direction (Schneider and Jensen 2008)

[d] Primary particle size after complete dispersion: 100–500 nm wide sheets with a thickness of app. 1 nm

[e] This is a general value for organoclays determined by nitrogen adsorption by BET (e.g., Kamena 2005)

[f] This study

mostly for a "test of principle". The 5 min compaction time was selected empirically as it was found to be the time after which the constant pressure volume change became negligible as perceived by the operator using the hand-press (description below). At that stage we assume that the powders had reached a stable or at least a metastable aggregate structure.

Powder compaction was completed using a home-built press-bench with digital read-out and a hand-controlled pressure-lever and could be controlled within ± 1 kg. Powder was loaded into a stainless steel cylinder (30 mm internal diameter and 40 mm deep). The cylinder was topped and gently tapped three times towards a table top to settle the powder. Excess powder was carefully scraped of to level with the cylinder top. Then the cylinder was capped with a plug (30 mm diameter), fitting the inner dimension of the cylinder and used to decrease the volume under uniaxial pressure. The initial bulk density and its change during compaction were determined from the mass of the powder loaded into the cylinder and the volume of the powder in the cylinder according to Eq. 2:

$$\rho_{\text{bulk}} = \frac{M}{((l_{\text{o}} - l_{\text{i}}) \cdot \pi \cdot r^2)}, \tag{2}$$

where ρ_{bulk} is the bulk density, M is the powder mass, r is the cylinder radius, l_{o} is the height of the initial powder (the cylinder depth) and l_{i} is the distance to the powder surface in the steel cylinder. The distance from the cylinder top and the powder surface was measured using a micrometre sliding gauge. Losses of powder to the compression plug and the inner surface of the steel cylinder above the compacted powders were assumed negligible and were not considered in calculation of the bulk density.

The single drop and rotating drum dustiness test system

Figure 1 shows photographs of the experimental set-up and the interior of the rotating drum tester employed for the dustiness testing. The system has previously been described by Schneider and Jensen (2008) where full details of the system can be obtained. In short, the rotating drum is made in stainless steel and is a downscaled version of the drum prescribed by the recently developed EN 15051-standard (CEN 2005; Liden 2006). The main reason for minimizing the rotating drum test system was to reduce the amount of

test material and enable handling and testing of powders with unknown toxicities inside a standard-size fume hood as well as facilitating safe and easy cleaning. The total volume of the current drum is 5.93 L. The cylindrical part is 4.8 L and has three symmetrically placed lifter vanes (2 cm × 22.5 cm) to lift and drop the powder parcels during rotation (Fig. 1b). All inner surfaces are polished to minimise surface adhesion and allow easy cleaning. Build-up of static electricity in the drum was prevented by grounding as also prescribed by EN 15051.

All experiments were conducted at 11 rpm and a horizontal flow rate of 11 lpm to obtain the same number of powder parcels falling per minute and average horizontal flow velocity in the cylinder as in the EN 15051 test, respectively. HEPA filtered air was supplied in excess at atmospheric pressure at the
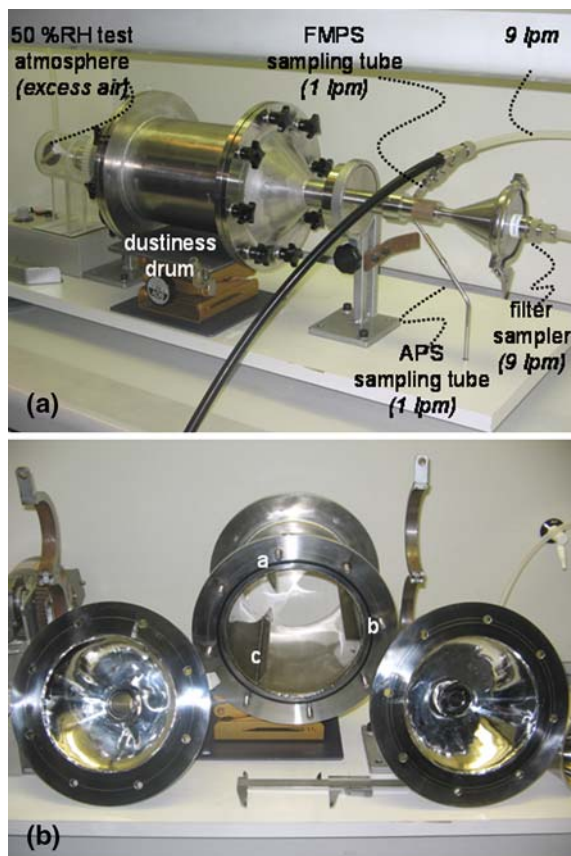

Fig. 1 Photographs of the rotating drum dustiness tester. (**a**) Photograph of the rotating drum mounted for dustiness testing. (**b**) Photograph showing the high-gloss polished inside of the dustiness drum. Also note the three lifter vanes marked a, b, and c at each 120° in the drum

drum inlet after conditioning to 50%RH as prescribed by EN 15051. At the other end of the drum, air was exhausted and distributed to the different sampling units (Fig. 1a).

The majority of the air (9 lpm) was passed to a Millipore membrane filter (0.8 µm pore size, 90 mm diameter) for particle collection. The mass of collected dust was determined in a conditioned weighing room (20 °C; 50%RH) using a Sartorius microbalance (Type R162 P; Sartorius GmbH, Göttingen, Germany). The detection limit (calculated as 3 times the standard deviation of blank filters) was 0.18 mg.

Additional 2 lpm air was collected an-isokinetically through two 3 mm inner diameter sharp edged probes at an angle of 45° (Fig. 1a). The first probe directed 1 lpm air sample vertically downwards through a two-stage dilution system (1:50) for particle measurement by an Aerodynamic time-of-flight Particle Sizer (APS) Model 3321 (TSI, Inc., MN, USA). The second probe directed 1 lpm air sample upwards to a Swagelock "T" where dilution air was added (1:10). Thereafter the air sample was led to a Fast Mobility Particle Sizer (FMPS) Model 3091 (TSI, Inc., MN, USA) through a conducting, flexible tube. All dilution air was HEPA filtered.

Theoretical calculations (Schneider and Jensen 2008) showed that the penetration efficiency of particles to the filter sampler closely resembled the curve for inhalable particles breathing through the nose in calm air and at moderate exercise (Dai et al. 2006). Hence, the particle mass collected on the filters corresponds to a fraction in between the thoracic and inhalable dustiness defined in EN 15051. The particle fraction collected by the APS was designed to mimic the thoracic fraction defined in CEN (1993).

Particle size distribution measurements of dust

Particle size distributions of fine and coarse particles were measured using the APS 3321, which measures the aerodynamic diameter, D_a. The particle sizing was based on measurements in 51 diameter classes with midpoints ranging from 0.52 to 18.43 µm. A separate class of particles smaller than 0.52 µm was also recorded but this size class was not used.

Nanoparticles and small submicrometre-size particles between 5.6 and 560 nm were measured by the FMPS. The FMPS measures particle sizes according to their electrical mobility diameter, D_m, in 32 diameter classes with midpoints ranging from 6.04 to 523 nm. To ensure stabilization of the FMPS, the system was turned on at least 30 min before zeroing of the electrometers. Both the APS and FMPS instruments were set to collect data at 1-s time resolution.

Study design

Before loading of powder, the exit cone of the drum was removed and the drum was oriented with a lifter vane placed at lowest position of the rotation circle. Six grams of powder was then carefully loaded in a pile on the upwards moving side at the centre of the lifter vane. Then, the system was closed, the humidity conditioned air-flow was applied, and all flows were checked. The experiment was then initiated by flushing the chamber with air for 180 s to reach background particle concentration levels and then performing a single-drop test by rotating the drum exactly 180° at 11 rpm. Then the drum was stopped for 180 s followed by 60 s of rotation, which was followed by 120 s of particle sampling without rotation. This completed the rotation part of the dustiness test. Hereafter the pump for filter collection and particle sampling was stopped and the filter sample was retrieved for weighing. After disassembling the drum, the remaining material was poured out and the material loosely adhered to the drum walls was removed by tapping on the drum as specified in EN 15051. The tips of the sampling probes for the FMPS and APS were cleaned by gently tapping the tube system towards the table top in the fume hood. The chamber of the standard cyclone Model 1031083 ($d_{50} = 1$ µm) delivered with FMPS was wiped with ethanol wetted, lint-free paper. The entire experimental cycle was repeated four times, where the first run served to saturate the internal surface of the drum (Burdett et al. 2000). When changing test-sample, the FMPS cyclone was cleaned completely and the grease on the bottom plate of the cyclone was replaced. When changing the test material, an additional cleaning procedure was implemented comprising wet wiping of the drum as well as complete cleaning of the cyclone coarse fraction chamber and replacing the grease on the bottom plate.

All materials were tested without further equilibration of the powders than what was achieved in the laboratory as also prescribed in EN 15051. However, some equilibration of adsorbed water will take place during the 180 s exposure to the 50%RH air in the

drum from the start to completion of the single-drop test. Differences in humidity affect the dustiness as determined by a continuous drop method (Plinke et al. 1995).

Data treatment

FMPS and APS number concentrations were exported as $dN/dlog_{10}D_p$-values for each particle size, D_p, using both Stoke's and specific density correction (Table 1). Despite the specific density cannot be expected to be the true density and the same over the whole size-spectrum of airborne particles studied, we anticipate that the specific density is closer to the real density than the standard density of 1 g/cm^3. Both the Stokes and density corrections were not used during measurements. Data from the single-drop and rotation testing were corrected for background based on the 40 s average size spectra sampled between 6 and 46 s before the single-drop test was initiated. For comparison the 20 s average was also calculated between 6 and 26 s before the concentration level started to rise in the rotation experiment. It was found that the two background concentrations were similar, suggesting that there was no accidental release of adhered dust remaining after the single-drop testing.

The total sum for each size channels was calculated based on all 1-s distribution spectra (i) for both the single-drop and the rotation test, using both the FMPS and the APS data:

$$\frac{dN_{single,sum}}{d \log D_p} = \sum_{i=t_{single}}^{i=t_{single}+120} \frac{dN_i}{d \log D_p} \left[cm^{-3}\right]$$

$$\text{and} \quad \frac{dN_{rotation,sum}}{d \log D_p} = \sum_{i=t_{rotation}}^{i=t_{rotation}+180} \frac{dN_i}{d \log D_p} \left[cm^{-3}\right],$$

$$(3)$$

The times, t_{single} and $t_{rotation}$, are the points in time where the particle concentration began to rise after start of the single-drop and rotation test, respectively. The single-drop and rotating drum test spectra obtained from Eq. 3 were fitted using a log-normal distribution to obtain the geometric mean diameter (GMD), geometric standard deviation (SD), and number concentration of each size mode (n_j). The FMPS and APS spectra were fitted with one and two modes, respectively.

The total number of generated particles, S, was calculated as:

$$S_{single} = \sum_j n_{j,single} \times Q$$

$$\text{or} \quad S_{rotation} = \sum_j n_{j,rotation} \times Q,$$

$$(4)$$

where j is the number of modes and Q is the total flow rate in cm^3 per second. S was calculated both for the single-drop and the rotation test, respectively, for both FMPS and APS data. The volume of respirable particles was calculated based on the mobility diameter for the FMPS data and the volume-equivalent diameter for the APS data and weighing according to the inhalation efficiency for respirable particles according to the respirable convention (CEN 1993).

The dust generation rate, R_i, in units of particle volume generated per second at time, i, was calculated using applied inverse digital filtering (Hjemsted and Schneider 1996). The equation is:

$$R_i = \frac{k}{\Delta t} \left(C_i - C_{i-1} e^{-\frac{\Delta t}{\tau}} \right),$$

$$(5)$$

where k is the drum volume, Δt is the time (1 s) between data points, C is the volume concentration, and τ is the measured time constant, which previously was shown to be 20 s (Schneider and Jensen 2008). C_i was calculated as the average of three runs, matched in time according to onset of the concentration rise. Only the APS data were used.

The dustiness index determined by the filter method was calculated as the total mass collected on the filter in mg divided by the mass of the test sample in kg. The mass determined on the filter sample was multiplied by a factor of 11/9 to adjust for the difference between the total volume flow (11 lpm) in the drum and the volume flow through the filter (9 lpm). The change in size distribution of particles sampled on the filter, which was caused by the an-isokinetic sampling for the FMPS and APS, was disregarded. For details, see Schneider and Jensen (2008).

Statistics

Statistical data analysis were made using Minitab 15 Statistical Software (Minitab Inc., Pennsylvania, USA). Comparison of the loose versus compacted powders of the same precursor was tested in a paired

two-tailed *t*-test. Statistical analysis of significant differences between the dustiness levels and ranking order for the different powder types was completed using an unstacked ANOVA Tukey one-way multiple comparison test of variance. Probabilities were calculated based on a confidence interval of 95 percent (95% CI) in both statistical models.

Results and discussion

Powders characteristics

Macroscopic analysis showed that the Bentonite and Nanofil®5 powders had different physical and textural characteristics. These differences may lead to different handling and dustiness properties.

The original Bentonite appeared as a loose creamy-white powder consisting of very fine to fine angular blocky agglomerates, which were up to app. 5 mm in size (Fig. 3a). The agglomerates had very low strength and were easily broken up by exerting a gentle pressure with a spatula or gently tapping the sample beaker. The actual physical dimensions of the individual Bentonite particles are unknown, but Rietveld analysis of powder X-ray diffraction data has shown that the average thickness of the individual clay-mineral sheets was 7.8 nm along the crystallographic [001] direction (Schneider and Jensen 2008). The bulk density was 0.75 g/cm^3 and in good agreement with previous analysis (Schneider and Jensen 2008). Since the typical specific density of montmorillonite is app. 2.1 g/cm^3, the porosity in the bulk powder was on the order of 64%.

The original Nanofil®5 appeared as a loose and slightly greasy creamy-white powder with a green tint. The powder mainly consisted of fine to very fine spherical nodules of up to app. 1 cm-size (Fig. 3b). Testing with a spatula, these granula had notably higher strength than the Bentonite agglomerates. The bulk density was 0.40 g/cm^3, whereas the specific density of the organoclay was given as 1.8 g/cm^3 (Table 1). Consequently, the porosity of the bulk organoclay powder was higher than for the Bentonite and about 78%.

The compacted samples naturally occurred as denser powders than their original precursors (Figs. 3c and d). The compaction test showed a large increase in the bulk density within the first 0.70 ± 0.14 kg/cm^2
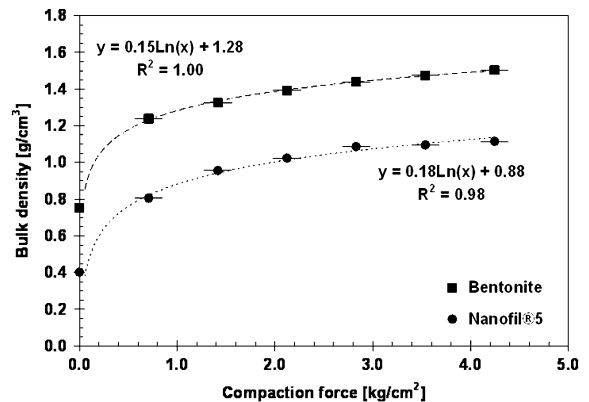

Fig. 2 Variation in bulk density plotted as function of compaction force for the Bentonite and Nanofil®5 powder in the uniaxial compaction cylinder test. Error bars are standard deviation of measurements based on four measurements at each pressure interval. The empirical bulk density functions were calculated omitting the un-compacted powders

uniaxial pressure (Fig. 2). Both powders showed a logarithmic increase in bulk density until maximum test loading at 4.24 ± 0.14 kg/cm^2. After compaction, both powders (Bentonite-C) and (Nanofil®5-C), the "C" denoting the compacted powder, formed solid plugs in the test cylinder.

The compacted samples used for dustiness testing were subjected to 3.54 ± 0.14 kg/cm^2 uniaxial pressure for 5 min and showed similar characteristics as observed for the powders at maximum loading. At 3.5 kg/cm^2, the bulk densities had increased to 1.48 ± 0.01 and 1.10 ± 0.01 g/cm^3 for the Bentonite-C and Nanofil®5-C, respectively. However, these values are not the bulk densities of the compacted powders used for dustiness testing, but that of the powder plugs, which at these compaction levels reached porosities of 29% and 38% for the Bentonite and Nanofil®5 powders, respectively. These density and porosity values may be close to those of the individual powder agglomerates.

The powders used for dustiness testing were scooped out of the stainless steel cylinder using a sampling spoon made of stainless steel. The compacted powder samples thereafter appeared as dense and fine to coarse angular to elongated agglomerates (granulates) of up to app. 2.3 cm in size along their maximum dimensions (Fig. 3c and d). The majority of the particle agglomerates were notably smaller with sizes below 0.5 cm in diameter. Noteworthy, the Bentonite-C aggregates appeared to have lower

Fig. 3 Photographs showing the macroscopic nature of the powder materials: (**a**) Bentonite; (**b**) Nanofil®5; (**c**) Compacted Bentonite (Bentonite-C); (**d**) Compacted Nanofil®5 (Nanofil®5-C). For scale, the black carbon rod is 0.5 mm in diameter
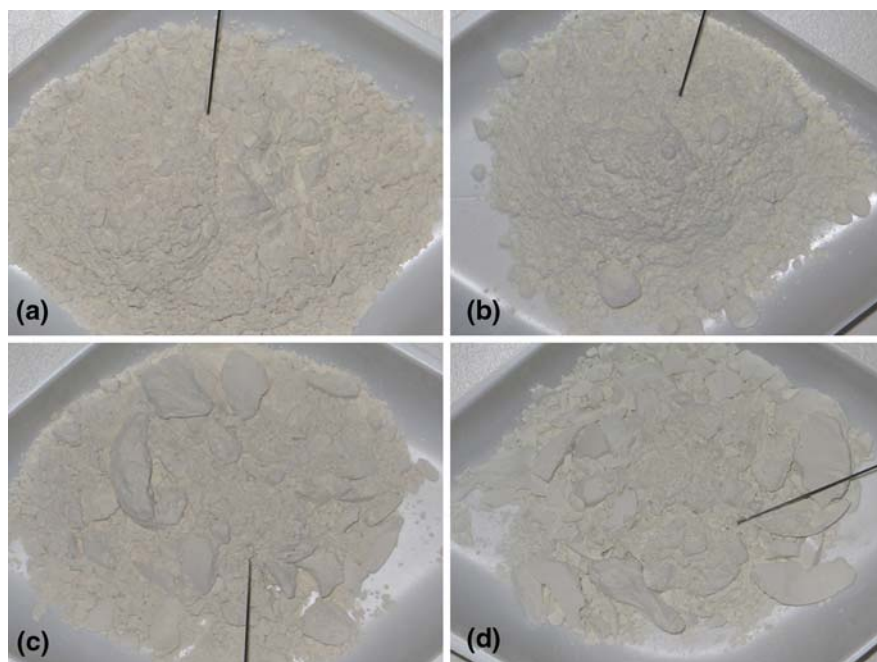
strength and broke up at a gentle, but lower pressure exerted with a spatula than Nanofil®5-C aggregates. The major physical difference between the compacted powders was the higher density and lower aggregate strength in the Bentonite-C aggregates compared to the Nanofil®5-C aggregates.

Particle size distributions

The dusts generated from testing of both the loose and compacted powders showed a multimodal particle size distribution. Figure 4 shows the 5-s average particle number-size distribution at the peak concentration during single-drop testing, as well as the 5-s average size distribution at the initial burst and at the end of the rotating drum testing. In Bentonite, we observed three modes with peaks at app. 300 nm, 1 μm, and 2.5 μm, respectively (Fig. 4a and b). These three modes enable satisfactory fitting of the particle size distribution profiles. The size-modes were slightly different in the dusts generated by the Nanofil®5 powders where the most prominent peaks occurred at almost 400 nm and at 1.2 μm (Fig. 4c and d). The modes belonging to the 300–400 nm peaks in the Bentonite and Nanofil®5 dusts were broad and started in the nm-range around 80 nm. Small nm-size peaks also appeared between 10 and

20 nm in the tests. Analysis of the raw data showed that these peaks could be explained by episodic fluctuations in the background in combination with noise from the electrometers. These factors may also explain the single channel peak which occasionally occurred below 10 nm in Fig. 4a–d. However, the single-drop test of Nanofil®5 showed a clear peak at app. 40 nm (Fig. 4c). Analysis of the individual runs showed that this peak was caused by one of the triplicate tests, which showed a very distinct bimodal size distribution in the FMPS size-range with a high-concentration size-mode at 25–34 nm and app. 250 nm, respectively. It thus cannot be excluded that Nanofil®5 powders may occasionally generate dust with nm-size particle modes.

The GMD of the size modes for compacted and loose powders was similar (Fig. 4b and d), excluding the 40-nm peak in Nanofil®5. However, differences were observed in the relative concentrations (n_j) of the size modes obtained, especially in the experiment with Nanofil®5 where the coarse size mode was reduced in the single-drop test of the compacted sample as compared to that in dust from the loose powder (Fig. 4d).

Several previous studies have reported an overall bimodal or trimodal particle size-distributions during aerosolization of various nanoparticle powders

Fig. 4 Stokes and density corrected 5-s average particle number size distributions of the dusts generated in the single-drop test (peak-concentration) and during the rotation test (after primary rise in concentration and 60 s into the experiment). (**a**) Bentonite; (**b**) Bentonite-C; (**c**) Nanofil®5; (**d**) Nanofil®5-C. Note that the axis in (**d**) is twice the value of the y-axis in (**a**, **b**, and **c**)
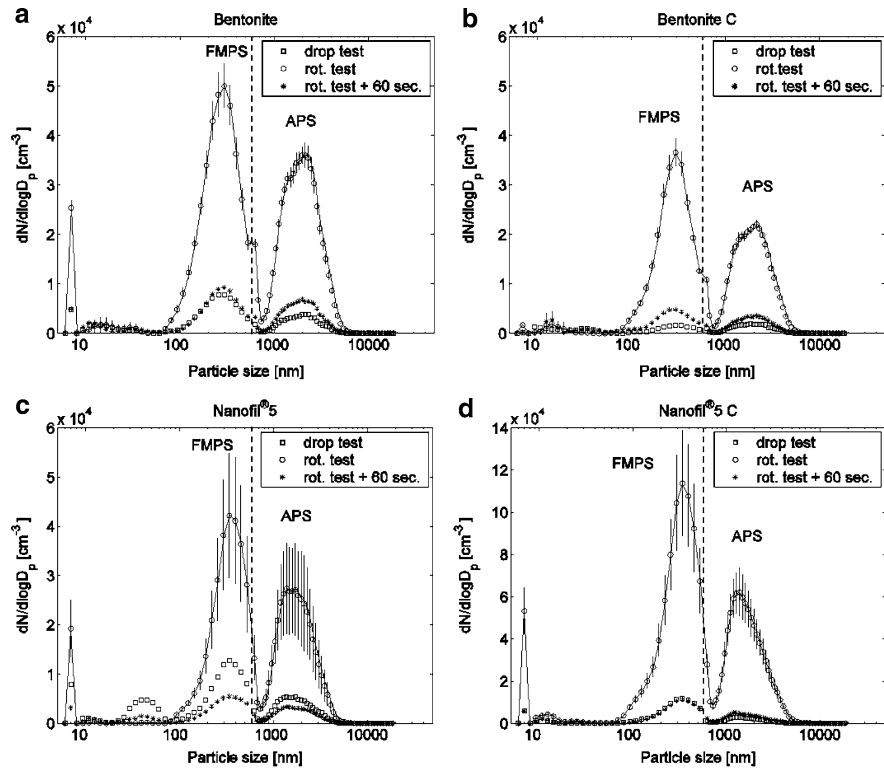
(Bohgard et al. 1994; Maynard et al. 2004; Kuhlbusch et al. 2004; Schneider and Jensen 2008). All these re-aerosolization experiments suggest that dust generated during handling of nanoparticle powders is mainly composed of particle agglomerates with bi- or multimodal size distributions and size-modes above 100 nm. In our current experiment, both particles had individual sheet thicknesses below 10 nm (8 nm for Bentonite and 1 nm for Nanofil®5). Except for the single triplet dustiness test with Nanofil®5, we were unable to identify particle size modes below 80 nm-size. This may in part be explained by the platy morphology where the dimensions perpendicular to [001] may vary from 100 nm to μm-size. For Nanofil®5, the width of the single organoclay sheets was listed as 100–500 nm (Table 1).

Previously, true nm-size modes have only been reported in powder re-aerosolization studies of single-walled carbon nanotubes, where a distinct nanoparticle mode was observed below 30 nm using a two-component vortex shaker fluidised bed method and measuring with a Scanning Mobility Particle Sizer (Maynard et al. 2004). Our present study

further substantiate that re-suspended dusts generated from nanoparticle powders are mainly released in agglomerates larger than 100 nm. Detailed understanding of the toxicological effects of agglomerates and single nanoparticles as well as agglomerate stability in physiological fluids is currently lacking (Maynard 2002). However, recent studies have shown that differences in toxicity and toxicological mechanisms may occur depending on the agglomeration state of nanoparticles (Limbach et al. 2005; Raja et al. 2007; Wick et al. 2007). Further understanding of these factors is important for reliable risk assessments of nanoparticle-based powder exposure.

Dustiness kinetics

Previously, three different particle volume generation rate time profiles have been identified: a brief initial burst, a slowly decreasing, and a constant generation rate (Schneider and Jensen 2008). In the present study, loose Nanoclay®5 and Bentonite showed a decreasing generation rate (Fig. 5a and b). The compacted Nanofil®5 powders showed a constant particle generation rate, as previously observed for

Fig. 5 Particle generation rate (S in Eq. 4) of the two clay powder samples in their initial state and their compressed form during rotating drum testing. (**a**) Loose and Compacted Bentonite. (**b**) Loose and compacted Nanofil®5
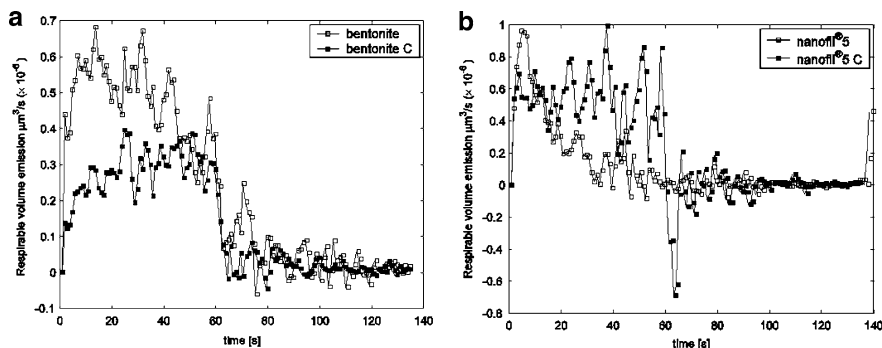
fumed silica and granulated zirconia (Schneider and Jensen 2008). Compacted Bentonite showed a new pattern in which there was a slowly increasing particle generation rate reaching a plateau towards the end of the rotating drum dustiness test (Fig. 5a). These different particle volume generation patterns and their levels are potentially important descriptors for the mechanisms of dust release during powder handling and may be used in the future for more accurate assessments of dust exposure in specific processes. In this study we observed a reduction in the rotating drum dustiness kinetics with compacted Bentonite. The initial dustiness kinetics of Nanofil®5-C was similar to that of the un-compacted organo-clay, but then remained almost constant and above the level obtained for the loose powders. Hence, both the size distribution and the kinetics of dust release were significantly affected by the compaction of Nanofil®5.

Dustiness levels

Table 2 lists the different measures employed for determination of the dustiness of the four powders and the results are plotted in Fig. 6. The mass-based dustiness index, which includes the dust generated during both the single-drop and rotating drum tests, shows that the loose and the compacted Bentonite released $2{,}077 \pm 317$ and $1{,}686 \pm 519$ mg dust per kg powder, respectively. Hence, the applied compaction level resulted in app. 20% reduction in the dustiness of Bentonite, which was found statistically near-significant ($p = 0.0833$; 95% CI; paired 2-tailed t-test). In the current study, the dustiness index for the loose Bentonite was 22% higher ($p = 0.0410$; 95% CI; paired 2-tailed t-test) than in the earlier test ($1{,}710 \pm 206$ mg/kg) conducted on the same material by Schneider and Jensen (2008) (Table 2). The difference may be caused by seasonal differences in

Table 2 Dustiness index and number of generated particles (mean $\pm$ SD) measured with the FMPS and APS in the single drop and rotating drum tests

Sample	Bentonite	Bentonite-C	Nanofil®**5**	Nanofil®5-C
Dustiness Index (mg/kg powder)				
Filter measurement[a]	$2{,}077 \pm 317$	$1{,}686 \pm 519$	$1{,}077 \pm 201$	$3{,}487 \pm 678$
Total number of generated particles				
FMPS (Single drop)	$2.12 \cdot 10^7 \pm 6.61 \cdot 10^6$	$6.62 \cdot 10^6 \pm 2.89 \cdot 10^6$	$2.05 \cdot 10^7 \pm 2.69 \cdot 10^6$	$2.19 \cdot 10^7 \pm 4.29 \cdot 10^6$
APS (single drop)	$1.72 \cdot 10^7 \pm 3.30 \cdot 10^6$	$4.13 \cdot 10^6 \pm 7.85 \cdot 10^5$	$1.92 \cdot 10^7 \pm 2.61 \cdot 10^6$	$9.35 \cdot 10^6 \pm 4.65 \cdot 10^5$
FMPS (rotation)	$2.98 \cdot 10^8 \pm 1.19 \cdot 10^7$	$1.90 \cdot 10^8 \pm 1.58 \cdot 10^7$	$1.72 \cdot 10^8 \pm 6.47 \cdot 10^7$	$5.88 \cdot 10^8 \pm 1.20 \cdot 10^8$
APS (rotation)	$2.40 \cdot 10^8 \pm 7.37 \cdot 10^6$	$1.34 \cdot 10^8 \pm 1.21 \cdot 10^7$	$1.34 \cdot 10^8 \pm 4.79 \cdot 10^7$	$3.31 \cdot 10^8 \pm 2.85 \cdot 10^7$
Change after compaction (%)				
Dustiness index	-19		$+224$	
FMPS/APS (single drop)	$-69/-76$		$+7/-51$	
FMPS/APS (rotation)	$-36/-44$		$+242/+147$	

[a] Value corresponds to a size fraction between the inhalable and thoracic fractions referred to in EN15051 and includes the dust generated in both the single-drop and rotation test
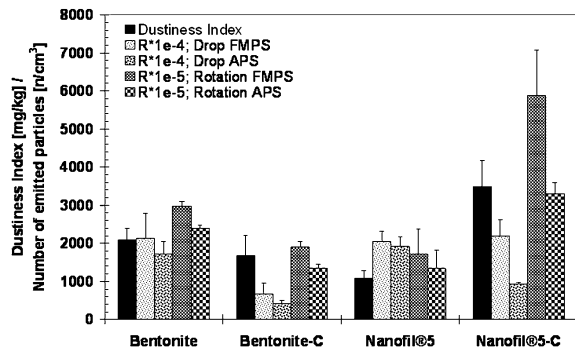
Fig. 6 Dustness index (mg/kg powder) obtained from the loose and compacted clay products compared with the corresponding total number (R) of generated respirable particles measured by the FMPS and APS during the single-drop and rotation testing. Note that for scaling, the FMPS and APS single drop R-values are multiplied by 10^{-4}, while the FMPS and APS rotating drum data are scaled by multiplying with 10^{-5}. Error bars show the standard deviation in the triplicate tests

laboratory humidity. Typical laboratory humidity levels may vary from 30 to 40%RH in winter (season for testing in this study) to 50–60%RH or even higher during summer (season for testing by Schneider and Jensen 2008). Regardless of these variations, all the Bentonite dustness indices were within the same moderate dustness class compared to the benchmark values obtained by Schneider and Jensen (2008).

Despite consisting of smaller individual crystal-lites and higher apparent porosity, the loose Nanofil®5 powder (1,077 ± 201 mg/kg) had notably lower dustness index than the loose Bentonite (2,077 ± 317 mg/kg). Schneider and Jensen (2008) found an overall increase in dustness with decreasing particle size. However, the differences in particle size and apparent porosity in the current powders were probably too small to make an effect and other material characteristics may be more important for these types of particles. It is likely that the abundant mm- to cm-size nodular agglomerates/granula may have caused the lower dustness index for Nanofil®5 (Fig. 3b). These granula were not observed in Bentonite (Fig. 3a).

In contrast to the loose powder, the compacted Nanofil®5 had the highest dustness index (3488 ± 678 mg/kg) of the tested powders. The mass-based dustness index was increased by more than 220% as compared to dustness of the loose Nanofil®5 powder ($p = 0.014$; 95% CI; paired two-tail t-test). Considering

that the dustness index obtained in our test only gives the fraction inhaled by nose-breathing, the dustness of Nanofil®5 approaches the high dustness index. In the EN 15051 standard, the dustness index of thoracic dust is moderate at 200–1,000 mg/kg and high if the dustness index exceeds 1,000 mg/kg. For inhalable dust, the medium level of dustness is defined between 1,000 and 5,000 mg/kg and high above 5,000 mg/kg powder.

Analysis of the dustness based on the total number of particles generated in the FMPS and APS size-ranges during both single-drop and rotating drum testing enables a more detailed understanding of the effects of compaction of these clay powders (Fig. 6). Even though the mass-based dustness index for Bentonite was reduced by app. 20%, compaction reduced the number of generated particles during single-drop testing by app. 70% in both the APS and FMPS particle ranges, respectively (Table 2). A slightly lower reduction in the number of generated particles (ca. 40%) was observed in the rotating drum test of Bentonite-C as compared to loose Bentonite powder. The greater decrease in respirable particle numbers suggests that the dustness index, which is closer to the inhalable fraction, is highly influenced by the coarser size fraction in Bentonite. Similarly, despite our observation of a higher mass-based dustness index for Nanofil®5-C as compared to the loose Nanofil®5 powder, compaction reduced the number of particles generated in the APS size-range by app. 50% in the single-drop test (Table 2; Fig. 6). The number of particles in the FMPS size range was almost the same. Hence, the increase in dustness only occurred during rotating drum testing, where the total number of particles increased by 242 and 147% in the FMPS and APS size-ranges, respectively (Table 2). Hence, compaction did reduce the dusti-ness of both Bentonite and Nanofil®5 powders in single-drop testing, but the dustness was increased in rotating drum testing of compacted Nanofil®5, in contrast to the behaviour of Bentonite. The increased dustness levels observed for the organoclay was an unexpected result as high-pressure compaction usu-ally is employed to reduce dustness of clay powders as explained in, e.g., Heim et al. (2005).

In the case of Nanofil®5, the reason for this effect is uncertain. The original aggregate structure may have been destroyed during compaction, and thereby caused higher dustness during repeated agitation of

the compacted Nanofil®5 as compared to the original loose powder. Thus, transferring the observations to handling, compaction could potentially decrease dust exposure during emptying a bag and increase potential exposure during mixing processes where powders are subjected to a number of agitations.

Considering the different dustness behaviour in single-drop and rotating drum testing, ranking of dustness of different powders may vary significantly depending on the different metrics used for the evaluation. We found the same relative ranking in the mass-based dustness index as in ranking the number of particles generated in the FMPS and APS modes during rotating drum testing:

Rotating drum

Dustness index: Nanofil®5$_{p=0.131}$ ≤ Bentonite-C$_{p=0.327}$ ≤ Bentonite$_{p=0.031}$ < Nanofil®5-C
FMPS: Nanofil®5$_{p=0.668}$ ≤ Bentonite-C$_{p=0.001}$ < Bentonite$_{p=0.014}$ < Nanofil®5-C
APS: Nanofil®5$_{p=1.000}$ = Bentonite-C$_{p<0.001}$ < Bentonite$_{p=0.006}$ < Nanofil®5-C

The p-values listed are the probabilities for the previous value being similar to the next value based on an unstacked ANOVA Tukey one-way multiple comparison test of variance. Even though ranking was similar between these three measures they are defined by markedly different levels of statistical significance of the ranking. All three metrics show almost similar dustness of Nanofil®5 and compacted Bentonite-C and significant differences were only observed between Bentonite-C, Bentonite, and Nanofil®5-C in the particle number analysis.

As may have been expected from the particle volume generation rate time profiles, ranking using the results from the single-drop tests showed a different order than the ranking according to rotating drum testing:

Single drop

FMPS: Bentonite-C$_{p=0.004}$ < Nanofil®5$_{p=0.869}$ ≤ Bentonite$_{p=0.881}$ ≤ Nanofil®5-C
APS: Bentonite-C$_{p=0.001}$ < Nanofil®5-C$_{p=0.015}$ < Bentonite$_{p=0.461}$ ≤ Nanofil®5

where the p-values were calculated as explained above. The greatest difference from the rotating drum test, as well as internally in the single-drop test, was

observed by the different ranking of loose and compacted Nanofil®5. This was caused by the relatively few particles generated in the APS-range. In the FMPS-size range, the number of particles generated was quite similar, except a significantly lower fine particle dustness of compacted Bentonite. Hence, the ranking was much clearer using the single-drop APS- than the FMPS-size range, where only the difference between Bentonite and Nanofil®5 was non-significant.

Hence, dustness evaluations based on the combination of particle concentrations, dustness kinetics and actual particle size distribution data appears to be a more informative tool than the mass-based determination based on traditional filter sampling alone. The statistical analyses of particle numbers appears more sensitive and statistically gives higher significance than comparisons of the mass-based dustness index. Moreover, more detailed information on the extent of fine or coarse dust can be achieved directly using the size distributions and number of particles generated. All in all these different outcomes are closely related to the dustness kinetics of the powders studied, which again is controlled by material properties in combination with production and storage conditions. Here we have shown that compaction may play an important role for the dustness kinetics and dustness levels, which also can induce great differences in the risk of exposure depending on specific use and handling techniques.

Conclusions

- Bi- or trimodal particle size distributions of aggregated and/or agglomerated particles were produced during dustness testing of montmorillonite-rich Bentonite and montmorillonite-based organoclay powders (Nanofil®5). The particle size modes in the dust had peaks between 300 and 400 nm as well as between 1.2 and 3 μm, despite the individual clay-mineral platelets being thinner than 10 nm. One test of Nanofil®5 showed an unusual size mode below 100 nm. This work supports previous studies suggesting that nanoparticle powders mainly produce dust clouds of agglomerated individual particles.
- The dustness index of loose Bentonite and Nanofil®5 powders were moderate and reached

2077 ± 317 and 1077 ± 201 mg/kg powder, respectively. Hence, the conversion from montmorillonite clay in Bentonite (8 nm thick; unknown width) to organically functionalised organoclay nanoflakes (1 nm thick; 100–500 nm wide) does apparently not increase dustiness. This may be explained by the differences in physical and textural characteristics of the powders. Especially the soapy nature and presence in nodular aggregates may reduce the dustiness as compared to the much looser agglomerates observed in the tested Bentonite.

- Low-pressure powder compaction increased the bulk density in a logarithmic manner and affected the dustiness index of Bentonite and organoclay powders compacted at 3.5 kg/cm^2. For Bentonite, the dustiness index was reduced by app. 20%, whereas the number of generated particles in the rotation test was reduced by app. 40%. The effect of compaction was just the opposite in the rotation test with Nanofil$^{\circledR}$5, where dustiness increased to app. 150–225%, depending on which measure was used. In single-drop testing, however, compaction resulted in equal or reduced dustiness, especially for coarse-size particles measured with the APS (50–75%). Hence, powder compaction may be a highly important parameter, which may affect the dustiness of powder and the resulting risks of exposure significantly.

- Combined with a previous study (Schneider and Jensen 2008), four types of particle volume generation rate time-profiles have been identified in rotating drum dustiness testing: initial burst, constant rate, slowly decreasing and slowly increasing, the latter being a new type observed in this work. In the future, these different dust generation time-profiles may be developed for detailed analysis of dustiness behaviour of powders and predict the dustiness levels in comparisons between single-drop and rotating drum testing as well as assessments of exposure risk during various types and durations of handling techniques.

References

Bohgard M, Anderberg MT, Eklund A (1994) Source characteristics of emitted aerosols in the size range 0.02 to 20 μm at pigment handling in dye manufacturing. J Aerosol Sci 25(Suppl 1):S461–S462

Brockel U, Wahl M, Kirsch R, Feise HJ (2006) Formation and growth of crystal bridges in bulk solids. Chem Eng Technol 29:691–695

Burdett GJ, Chung KYK, Mark D, Armbruster L, Breum NO (2000) Development of a method for dustiness testing. EU contract SMT4-CT96-2074. HSE report IR/L/MF/00/11. Health and Safety Laboratory, Sheffield, UK

Carrizosa MJ, Hermosin MC, Koskinen WC, Cornejo J (2003) Use of organosmectites to reduce leaching losses of acidic herbicides. Soil Sci Soc Am J 67:511–517

CEN (1993) EN 481. Workplace atmospheres—size fraction definitions for measurements of airborne particles. European Committee for Standardization, Brussels

CEN (2006) EN 15051 Workplace atmospheres–Measurement of the dustiness of bulk materials—requirements and reference test methods. European Committee for Standardization, Brussels

Dai Y-Y, Juang Y-J, Wu Y-Y, Breysse PN, Hsu D-J (2006) In vivo measurement of inhalability of ultralarge aerosol particles in calm air by humans. J Aerosol Sci 37:967–973

Freitag F, Kleinebudde P (2003) How do roll compaction/dry granulation affect the tableting behaviour of inorganic materials? Comparison of four magnesium carbonates. EJPS 19:281–289

Gbureck U, Dembski S, Thull R, Barralet JE (2005) Factors influencing calcium phosphate cement shelf-life. Biomaterials 26:3691–3697

Guven N (1991) On a definition of Illite Smectite mixed-layer. Clays Clay Miner 39:661–662

Heim A, Obraniak A, Gluba T (2005) Changes of feed bulk density during drum granulation of Bentonite. Physicochem Probl Miner Process 39:219–228

Hjemsted K, Schneider T (1996) Documentation of a dustiness drum test. Ann Occup Hyg 40:627–643

Kamena K (2005) Nanoclays and their emerging markets. In: Xanthos M (ed) Functional fillers for plastics. WILEY-VCH Verlag GmbH & Co. KGaA, Weinheim, pp 163–174

Konta J (1995) Clay and man: clay raw materials in the service of man. Appl Clay Sci 10:275–335

Kuhlbusch TAJ, Neumann S, Fissan H (2004) Number size distribution, mass concentration, and particle composition of PM_1, $PM_{2.5}$, and PM_{10} in bag filling areas of carbon black production. J Occup Environ Hyg 1:660–671

Liden G (2006) Dustiness testing of materials handled at workplaces. Ann Occup Hyg 50:437–439

Limbach LK, Li YC, Grass RN et al (2005) Oxide nanoparticle uptake in human lung fibroblasts: effects of particle size, agglomeration, and diffusion at low concentrations. Environ Sci Technol 39:9370–9376

Maynard AD (2002) Experimental determination of ultrafine TiO$_2$ deagglomeration in a surrogate pulmonary surfactant: preliminary results. Ann Occup Hyg 46(Supplement 1):197–202

Maynard AD, Baron PA, Foley M et al (2004) Exposure to carbon nanotube material: aerosol release during the

handling of unrefined single-walled carbon nanotube material. J Toxicol Environ Health A 67:87–107

Nishii K, Horio M (2007) Dry granulation. In: Salman AD (ed) Handbook of powder granulation technology, Chap 6. Elsevier Science B.V., pp 289–322

Patel HA, Somani RS, Bajaj HC, Jasra RV (2006) Nanoclays for polymer nanocomposites, paints, inks, greases and cosmetics formulations, drug delivery vehicle and waste water treatment. Bull Mater Sci 29:133–145

Plinke MAE, Leith D, Boundy MG, Löffler F (1995) Dust generation from handling powders in industry. Am Ind Hyg Assoc J 56:251–257

Raja PMV, Connolley J, Ganesan GP et al (2007) Impact of carbon nanotube exposure, dosage and aggregation on smooth muscle cells. Toxicol Lett 169:51–63

Ray SS, Okamoto M (2003) Polymer/layered silicate nano-composites: a review from preparation to processing. Prog Polym Sci 28:1539–1641

Schneider T, Jensen KA (2008) Combined single-drop and rotating drum dustiness test of fine to nanosize powders using a small drum. Ann Occup Hyg 52/1:23–34

Szepvolgyi J, Mohai I, Gubicza J (2001) Atmospheric ageing of nanosized silicon nitride powders. J Mater Chem 11:859–863

Takano K, Horio M (2004) Particle design for dry powder inhalation via binderless powder coating by pressure swing granulation. Powder Technol 141:196–202

Tardos GI (2005) Wet-granulation research with application to scale-up. China Particuol 3:191–195

Tien YM, Wu PL, Chu CA et al (2007) The friction-free compressibility curve of Bentonite block. Phys Chem Earth Parts A/B/C 32:809–819

Wick P, Manser P, Limbach LK et al (2007) The degree and kind of agglomeration affect carbon nanotube cytotoxicity. Toxicol Lett 168:121–131

Wieczorek M, Krysztafkiewicz A, Jesionowski T (2003) Comparative characteristics of local and foreign bentonites. Macromol Symp 194:345–350